

Tunable hydrogen storage in magnesium–transition metal compounds: First-principles calculations

Süleyman Er,¹ Dhirendra Tiwari,¹ Gilles A. de Wijs,² and Geert Brocks¹

¹*Computational Materials Science, Faculty of Science and Technology and MESA+ Research Institute, University of Twente, P.O. Box 217, 7500 AE Enschede, The Netherlands*

²*Electronic Structure of Materials, Institute for Molecules and Materials, Faculty of Science, Radboud University Nijmegen, Heyendaalseweg 135, 6525 AJ Nijmegen, The Netherlands*

(Received 13 October 2008; revised manuscript received 5 December 2008; published 9 January 2009)

Magnesium dihydride (MgH_2) stores 7.7 wt % hydrogen but it suffers from a high thermodynamic stability and slow (de)hydrogenation kinetics. Alloying Mg with lightweight transition metals (TM) ($=\text{Sc, Ti, V, Cr}$) aims at improving the thermodynamic and kinetic properties. We study the structure and stability of $\text{Mg}_x\text{TM}_{1-x}\text{H}_2$ compounds, $x=[0-1]$, by first-principles calculations at the level of density functional theory. We find that the experimentally observed sharp decrease in hydrogenation rates for $x \geq 0.8$ correlates with a phase transition of $\text{Mg}_x\text{TM}_{1-x}\text{H}_2$ from a fluorite to a rutile phase. The stability of these compounds decreases along the series Sc, Ti, V, and Cr. Varying the TM and the composition x , the formation enthalpy of $\text{Mg}_x\text{TM}_{1-x}\text{H}_2$ can be tuned over the substantial range of 0–2 eV/f.u. Assuming however that the alloy $\text{Mg}_x\text{TM}_{1-x}$ does not decompose upon dehydrogenation, the enthalpy associated with reversible hydrogenation of compounds with a high magnesium content ($x=0.75$) is close to that of pure Mg.

DOI: [10.1103/PhysRevB.79.024105](https://doi.org/10.1103/PhysRevB.79.024105)

PACS number(s): 71.20.Be, 71.15.Nc, 61.66.Dk, 61.50.Lt

I. INTRODUCTION

Hydrogen is a clean energy carrier and an alternative to carbon based fuels in the long run.¹ Mobile applications require a compact, dense, and safe storage of hydrogen with a high-rate loading and unloading capability.^{2,3} Lightweight metal hydrides could satisfy these requirements.^{4,5} Metal hydrides are formed by binding hydrogen atoms in the crystal lattice, resulting in very high volumetric densities. Reasonable hydrogen gravimetric densities in metal hydrides can be achieved if lightweight metals are used.

MgH_2 has been studied intensively since it has a relatively high hydrogen gravimetric density of 7.7 wt %. Bottlenecks in the application of MgH_2 are its thermodynamic stability and slow (de)hydrogenation kinetics. These lead to excessively high operating temperatures (573–673 K) for hydrogen release.^{6–8} The hydrogen (de)sorption rates can be improved by decreasing the particle size down to nanoscales.^{9–11} It is predicted that particles smaller than 1 nm have a markedly decreased hydrogen desorption enthalpy, which would lower the operating temperature.¹² The production of such small particles is nontrivial, however, and the hydrogen (de)sorption rates of larger nanoparticles are still too low.

An additional way of improving the (de)hydrogenation kinetics of MgH_2 is to add transition metals (TMs).^{9,13–15} Usually only a few wt % is added since TMs are thought to act as catalysts for the dissociation of hydrogen molecules. Recently however, Notten and co-workers^{16–26} have shown that the (de)hydrogenation kinetics is markedly improved by adding more TM and making alloys $\text{Mg}_x\text{TM}_{(1-x)}$, with TM = Sc and Ti, and $x \leq 0.8$. The basic ansatz is that the rutile crystal structure of MgH_2 enforces an unfavorably slow diffusion of hydrogen atoms.²⁷ ScH_2 and TiH_2 have a fluorite structure, which would be more favorable for fast hydrogen kinetics. By adding a sufficiently large fraction of these TMs,

one could force the $\text{Mg}_x\text{TM}_{(1-x)}$ compound to adopt the fluorite structure.

In this paper we examine the structure and stability of $\text{Mg}_x\text{TM}_{(1-x)}\text{H}_2$, with TM = Sc, Ti, V, and Cr, compounds by first-principles calculations. In particular, we study the relative stability of the rutile versus the fluorite structures. This paper is organized as follows. In Sec. II we discuss the computational details. The calculations are benchmarked on the TMH_2 simple hydrides. The structure and formation enthalpies of the compounds $\text{Mg}_x\text{TM}_{(1-x)}\text{H}_2$ are studied in Sec. III and an analysis of the electronic structure is given. We discuss the hydrogenation enthalpy of the compounds in Sec. IV and summarize our main results in Sec. V.

II. COMPUTATIONAL METHODS AND TEST CALCULATIONS

We perform first-principles calculations at the level of density-functional theory (DFT) with the PW91 functional as the generalized gradient approximation (GGA) to exchange and correlation.²⁸ As transition metals have partially filled $3d$ shells, we include spin polarization and study ferromagnetic and simple antiferromagnetic orderings where appropriate. A plane wave basis set and the projector augmented wave (PAW) formalism are used,^{29,30} as implemented in the VASP code.^{31,32} The cutoff kinetic energy for the plane waves is set at 650 eV. The total energies of MgH_2 , TMH_2 , and the hydrogen molecule are then converged to within 1 meV. Standard frozen-core potentials are applied for all the elements except for Sc, where we include $3s$ and $3p$ as valence shells, in addition to the usual $4s$ and $3d$ shells. The Brillouin zone (BZ) is integrated using a regular \mathbf{k} -point mesh with a spacing of $\sim 0.02 \text{ \AA}^{-1}$ and the Methfessel-Paxton scheme with a smearing parameter of 0.1 eV.³³ The self-consistency convergence criterion for the energy difference between two consecutive electronic steps is set to 10^{-5} eV. Structural optimi-

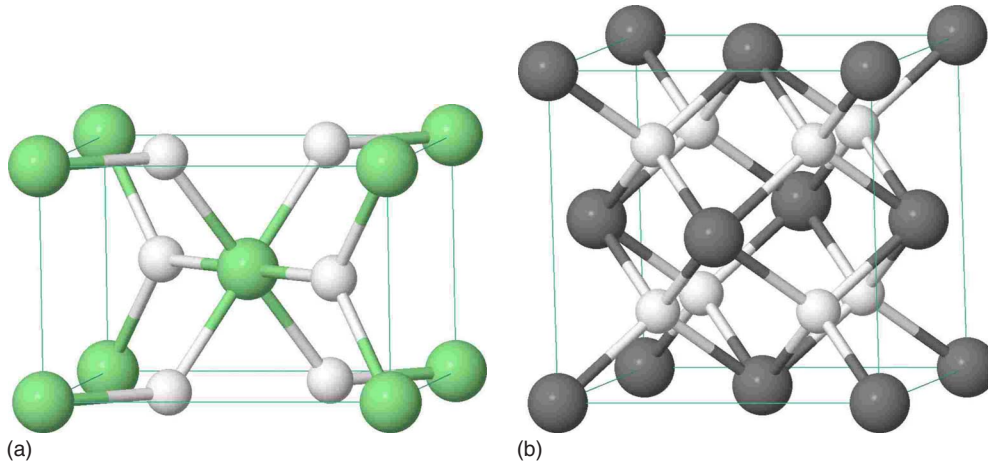
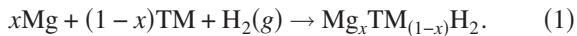


FIG. 1. (Color online) (Left) rutile crystal structure of α -MgH₂ and (right) fluorite crystal structure of α -TMH₂. The white spheres represent the hydrogen atoms.

zation is assumed to be complete when the total force acting on each atom is smaller than 0.01 eV/Å. The volumes of the unit cells are relaxed, and, where appropriate, also their shapes. Finally, we calculate accurate total energies for the optimized geometries using the tetrahedron method.³⁴

To calculate the formation enthalpies of the metal hydrides, we consider the following reaction.



The formation enthalpies (at $T=0$) are then obtained by subtracting the total energies of the reactants from that of the product. A cubic box of size 10 Å is applied for the H₂ molecule. The calculated H-H bond length, binding energy, and vibrational frequency are 0.748 Å, -4.56 eV, and 4351 cm⁻¹, respectively, in good agreement with the experimental values of 0.741 Å, -4.48 eV, and 4401 cm⁻¹.^{35,36}

Since hydrogen is a light element, the zero-point energy (ZPE) due to its quantum motion is not negligible. We find that the correction to the reaction enthalpies of Eq. (1) resulting from the ZPEs is 0.15 ± 0.05 eV/H₂, as function of the composition x and the transition metal TM. Since we are mainly interested in relative formation enthalpies, we omit the ZPE energy correction in the following.

Before discussing the Mg_xTM_(1-x)H₂ compounds, we benchmark our calculations on the simple compounds MgH₂ and TMH₂. Under standard conditions magnesium dihydride has the rutile structure α -MgH₂ (see Fig. 1) with space-group $P4_2/mnm$ (136), and Mg and H atoms in the $2a$ and $4f$ ($x=0.304$) Wyckoff positions, respectively. Each Mg atom is coordinated octahedrally by H atoms with two Mg-H distances of 1.94 Å and four distances of 1.95 Å. First row early transition-metal hydrides crystallize in the fluorite structure α -TMH₂ (see Fig. 1) with space-group $Fm\bar{3}m$ (225), and TM atoms in $4a$ and H atoms in $8c$ Wyckoff positions. Each TM has a cubic surrounding of H atoms with calculated TM-H bond lengths of 2.07, 1.92, 1.82, and 1.79 Å for Sc, Ti, V, and Cr, respectively. By breaking the cubic symmetry by hand and reoptimizing the geometry, we

have confirmed that the fluorite structure indeed represents a stable minimum.

The optimized cell parameters and the calculated formation enthalpies of the simple hydrides are given in Table I. The structural parameters are in good agreement both with available experimental data and with previous DFT calculations.³⁷⁻³⁹ The formation enthalpies of MgH₂ and VH₂ are somewhat underestimated by the calculations, whereas those of ScH₂ and TiH₂ are in excellent agreement with experiment. CrH₂ is predicted to be unstable with respect to decomposition.

III. RESULTS Mg_xTM_(1-x)H₂

A. Structures and formation enthalpies

Mg_xTM_(1-x)H₂ has the fluorite structure for $x=0$ and the rutile structure for $x=1$. We want to establish which of the

TABLE I. Optimized cell parameters a (c) and calculated formation enthalpies E_f of elemental dihydrides in their most stable (α) forms. All TMH₂ have a fluorite structure, with space-group $Fm\bar{3}m$ (225), whereas MgH₂ has a rutile structure, with space-group $P4_2/mnm$ (136).

Compound	a (c) (Å)		E_f (eV/f.u.)	
	Calc	Exp	Calc	Exp
MgH ₂	4.494(3.005)	4.501(3.010) ^a	-0.66	-0.76
ScH ₂	4.775	4.78 ^b	-2.09	-2.08
TiH ₂	4.424	4.454 ^c	-1.47	-1.45
VH ₂	4.210	4.27 ^d	-0.65	-0.79
CrH ₂	4.140	3.861 ^d	+0.13 ^e	

^aReference 40.

^bReference 41.

^cReference 42.

^dReference 43.

^eAntiferromagnetically ordered.

two structures is most stable at intermediate compositions x . First we summarize the current status of the experimental work on $\text{Mg}_x\text{TM}_{(1-x)}$ alloys.

Experimentally it has been demonstrated that $\text{Mg}_x\text{Sc}_{(1-x)}$ alloys can be reversibly hydrogenated, both in thin films as well as in bulk form.^{16,17,19,20,44,45} Mg and Ti do not form a stable bulk alloy, but thin films of $\text{Mg}_x\text{Ti}_{(1-x)}$ have been made, which are readily and reversibly hydrogenated.^{21–26,46} Thin films of $\text{Mg}_x\text{V}_{(1-x)}$ and $\text{Mg}_x\text{Cr}_{(1-x)}$ can also be easily hydrogenated.¹⁷ Attempts to produce nonequilibrium bulk $\text{Mg}_x\text{Ti}_{(1-x)}$ alloys by ball milling of Mg and Ti or their hydrides have had a limited success so far.^{47–50} However, Mg_7TiH_y crystals have been made using a high-pressure anvils technique.⁵¹ The same technique has been applied to produce the hydrides Mg_6VH_y and Mg_3CrH_y .^{52–54}

The crystal structure of $\text{Mg}_x\text{Sc}_{(1-x)}\text{H}_y$ and $\text{Mg}_x\text{Ti}_{(1-x)}\text{H}_y$ in thin films, $x \leq 0.8$, $y \approx 1-2$, is cubic, with the Mg and TM atoms at fcc positions. No detectable regular ordering of Mg and TM atoms at these positions has been found.^{23,44,45} In contrast, the Mg and TM atoms form simple ordered structures in the high-pressure phases.^{51–55} The hydrogen atoms in $\text{Mg}_{0.65}\text{Sc}_{0.35}\text{H}_y$, $y \approx 1-2$, assume tetrahedral interstitial positions, as is expected for the fluorite structure.^{44,45} In the $\text{Mg}_7\text{TiH}_{16}$ high-pressure phase, the metal atoms are in fcc positions and are ordered as in the Ca_7Ge structure.⁵¹ The H atoms are in interstitial sites but displaced from their ideal tetrahedral positions.⁵⁵

The latter structure can be used as a starting point to construct simple fluorite-type structures for $\text{Mg}_x\text{TM}_{(1-x)}\text{H}_2$, $0 < x < 1$. For $x=0.125, 0.875$ we use the Ca_7Ge structure, for $x=0.25, 0.75$ the Cu_3Au ($L1_2$) structure, and for $x=0.5$ the CuAu ($L1_0$) structure to order the metal atoms. The H atoms are placed at or close to tetrahedral interstitial positions. As the atomic volumes of the various TM atoms differ, in each of the structures and compositions, the cell parameters are optimized as well as the positions of all atoms within the cell. Care is taken to allow for breaking the symmetry in the atomic positions. In particular the hydrogen atoms are often displaced from their ideal tetrahedral positions. Although these structures are then no longer ideal fluorite structures anymore, we still use the term fluorite in the following. To model $\text{Mg}_x\text{TM}_{(1-x)}\text{H}_2$ in rutile-type structures we use the $\alpha\text{-MgH}_2$ structure as a starting point. We replace a fraction x of the Mg atoms by TM atoms and use the smallest supercell of the rutile structure where this leads to an integer number of atoms. In case of multiple possible cells, the results given below refer to the cell that leads to the lowest energy. Again we allow for symmetry breaking, and optimize the cell parameters and the atomic positions.

To assess the effect of disorder in the positions of the metal atoms, we performed test calculations on special quasirandom structures of $\text{Mg}_x\text{Ti}_{(1-x)}\text{H}_2$, which enable modeling of random alloys in a finite supercell. For instance, we use a 32 atom supercell to model quasirandom structures of fcc $\text{Mg}_x\text{Ti}_{1-x}$ for $x=0.25, 0.5$, and 0.75 , and a 64 atom supercell for $x=0.125$ and 0.875 .⁵⁶ Inserting hydrogen atoms in tetrahedral interstitial positions then gives supercells with a total number of atoms of 96 and 192, respectively. The cell parameters are optimized as well as the atomic positions.⁵⁷ The formation energies according to Eq. (1) of $\text{Mg}_x\text{Ti}_{(1-x)}\text{H}_2$ in

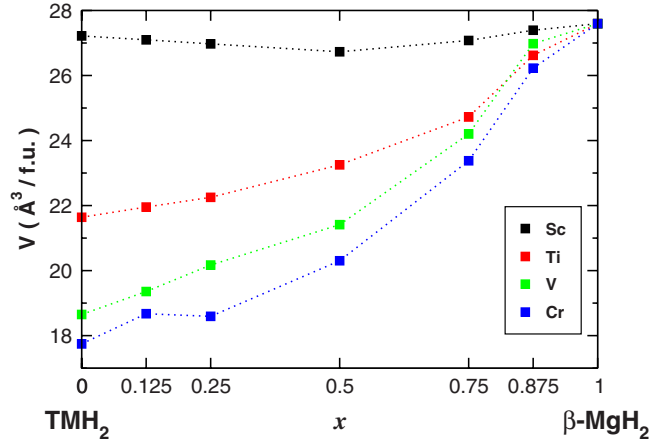


FIG. 2. (Color online) The volumes per formula unit in Å^3 of $\text{Mg}_x\text{TM}_{(1-x)}\text{H}_2$ in the fluorite structure, as a function of the composition x for $\text{TM}=\text{Sc}, \text{Ti}, \text{V},$ and Cr (from top to bottom).

these quasirandom structures are within ~ 0.1 eV/f.u. lower than those of the simple ordered structures. In particular, the relative stability of the fluorite vs the rutile structures is not sensitive to the relative ordering of the metal atoms. It is reasonable to expect that this also holds for the other $\text{Mg}_x\text{TM}_{(1-x)}\text{H}_2$ compounds.

The calculated volumes $V(\text{Mg}_x\text{TM}_{(1-x)}\text{H}_2)$ of the (simple) fluorite structures, normalized per formula unit (f.u.), are shown in Fig. 2. The volumes of the quasirandom structures of $\text{Mg}_x\text{Ti}_{(1-x)}\text{H}_2$ are within 1% of those of the simple structures. The volumes of a few bulk compounds and compositions can be extracted from experimental data, thus providing a check on the calculations. Interpolating the results in Ref. 44 gives $V(\text{Mg}_{0.65}\text{Sc}_{0.35}\text{H}_2)=27.5 \text{ Å}^3$, whereas the interpolated calculated value from Fig. 2 is 26.9 Å^3 . Reference 55 gives $V(\text{Mg}_{0.875}\text{Ti}_{0.125}\text{H}_2)=27.3 \text{ Å}^3$, compared to the calculated value 26.6 Å^3 . These differences between experimental and calculated volumes are consistent with the differences between experimental and calculated lattice parameters of the simple hydrides (see Table I). Experiments on thin films give $V(\text{Mg}_{0.7}\text{Ti}_{0.3}\text{H}_2)=26.4 \text{ Å}^3$, if one assumes cubic symmetry.²³ The interpolated computational value is 24.4 Å^3 . The difference between these values is not excessively large but considering the smaller difference found for the bulk composition $\text{Mg}_{0.875}\text{Ti}_{0.125}\text{H}_2$, it may suggest that the structure of thin films is slightly different from that of bulk.

The trends observed in Fig. 2 can be interpreted straightforwardly. The cell volumes of $\alpha\text{-ScH}_2$ and the cubic $\beta\text{-MgH}_2$ structure⁵⁸ are within 1.4% of one another, which explains why the volumes calculated for $\text{Mg}_x\text{Sc}_{(1-x)}\text{H}_2$ only weakly depend on the composition x . The cell volumes of the other TMH_2 are smaller; hence one expects the volumes $V(\text{Mg}_x\text{TM}_{(1-x)}\text{H}_2)$ to increase with x . At fixed composition x , the volumes $V(\text{Mg}_x\text{TM}_{(1-x)}\text{H}_2)$ decrease along the series Sc, Ti, V, and Cr, as the atomic volumes of the TMs decrease correspondingly. According to Zen's law of additive volumes, one would expect⁵⁹

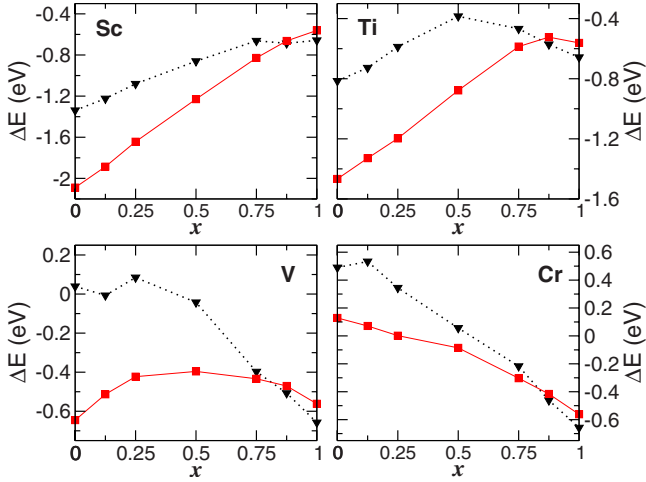


FIG. 3. (Color online) The formation enthalpy (per formula unit) of the $\text{Mg}_x\text{TM}_{(1-x)}\text{H}_2$ compounds as obtained from spin-polarized calculations. The values for the fluorite and rutile structures are represented by squares (solid lines) and triangles (dashed lines), respectively.

$$V(\text{Mg}_x\text{TM}_{(1-x)}\text{H}_2) = xV(\beta\text{-MgH}_2) + (1-x)V(\text{TMH}_2). \quad (2)$$

The curves shown in Fig. 2 deviate slightly, but distinctly, from straight lines with a maximum deviation of $\sim 5\%$. This deviation is consistent with the experimental observations on $\text{Mg}_x\text{Ti}_{(1-x)}\text{H}_2$.^{21,23} It is also observed in simple metal alloys.⁵⁹

The calculated formation enthalpies of $\text{Mg}_x\text{TM}_{(1-x)}\text{H}_2$ are shown in Fig. 3. Clearly for all TMs the fluorite structure is more stable than the rutile structure for all x smaller than a critical value, x_c . The critical composition x_c at which the rutile structure becomes more stable, as obtained by interpolation in Fig. 3, is in the range $x_c \approx 0.8-0.85$ for all TMs. The exact position of the critical composition x_c depends somewhat on the details of the structure. For quasirandom structures of $\text{Mg}_x\text{Ti}_{(1-x)}\text{H}_2$ the critical composition is at $x_c = 0.875$.⁵⁷ The fact that the critical composition is fairly high might be guessed from the energies of the fluorite and rutile structures of the simple hydrides. As a first estimate of the critical composition x_c below which the fluorite structure is stable, one may try a linear interpolation between the pure TMH_2 compounds, $x=0$, and MgH_2 , $x=1$. The rutile structure of TMH_2 is more unstable than the fluorite structure by $\Delta(\text{TMH}_2) = 0.75, 0.65, 0.68, \text{ and } 0.36$ eV/f.u. for $\text{TM} = \text{Sc}, \text{Ti}, \text{V}, \text{ and } \text{Cr}$, respectively. The difference in formation enthalpy between the α (rutile) and β (cubic) phases of MgH_2 is $\Delta(\text{MgH}_2) = 0.10$ eV/f.u. Linear interpolation then gives $x_c = \Delta(\text{TMH}_2) / [\Delta(\text{TMH}_2) + \Delta(\text{MgH}_2)]$, which results in $x_c \approx 0.9$ for Sc, Ti, and V, and $x_c = 0.8$ for Cr. Whereas these values may seem a good first guess, they are somewhat too high as compared to the crossing points x_c observed in Fig. 3. Moreover, as this figure shows, in particular the curves for Ti and V are far from linear so the results for the linear interpolation may be somewhat fortuitous.

Experimental results indicate that $\text{Mg}_{0.7}\text{Ti}_{0.3}\text{H}_2$ has the fluorite structure and $\text{Mg}_{0.9}\text{Ti}_{0.1}\text{H}_2$ has the rutile structure.²³ This agrees with the results shown in Fig. 1, where a fluorite to rutile phase transition takes place at the composition $x = x_c \approx 0.83$. It has been suggested that the fluorite structure allows for a much faster kinetics of hydrogen loading and unloading. Experimentally it has been observed that the dehydrogenation kinetics of $\text{Mg}_x\text{Sc}_{(1-x)}$ and $\text{Mg}_x\text{Ti}_{(1-x)}$ becomes markedly slower if $x \geq x_0 = 0.8$. The results shown in Fig. 1 suggest that $x_0 = x_c$, i.e., the composition at which the phase transition between fluorite and rutile structures takes place.

The dehydrogenation kinetics of $\text{Mg}_x\text{Ti}_{(1-x)}$ also becomes gradually slower with decreasing x , for $x < x_c$, i.e., where the compound remains in the fluorite structure, although it is still faster than for $x > x_c$.^{19,21} Whereas kinetic studies are beyond the scope of the present paper, we speculate that a volume effect might play a role here. In the fluorite structure the hydrogen atoms occupy interstitial positions close to the tetrahedral sites. Diffusion of hydrogen atoms is likely to take place via other interstitial sites such as the octahedral sites. The smaller the volume, the shorter the distance between such sites and the occupied positions, or in other words, the shorter the distance between a diffusing hydrogen atom and other hydrogen atoms in the lattice. This may increase the barrier for diffusion. As the volume of $\text{Mg}_x\text{V}_{(1-x)}$ and $\text{Mg}_x\text{Cr}_{(1-x)}$ is smaller than that of $\text{Mg}_x\text{Sc}_{(1-x)}$ and $\text{Mg}_x\text{Ti}_{(1-x)}$ (at the same composition x), this might also explain why the dehydrogenation kinetics of the former compounds is much slower.¹⁷ We note that the smaller volume of $\text{Mg}_x\text{V}_{(1-x)}$ and $\text{Mg}_x\text{Cr}_{(1-x)}$ is accompanied by a distortion of the structures consistent with the limited space available to accommodate the hydrogen atoms. For instance, in $\text{Mg}_{0.75}\text{V}_{0.25}\text{H}_2$ and $\text{Mg}_{0.75}\text{Cr}_{0.25}\text{H}_2$ the hydrogen atoms are displaced considerably from the tetrahedral positions, and the coordination number of V and Cr (by hydrogen) is seven instead of eight, as in case of a perfect fluorite structure.

B. Electronic structure

To analyze the electronic structure of the compounds $\text{Mg}_x\text{TM}_{(1-x)}\text{H}_2$, we start with the density of states (DOS) of the pure hydrides $\alpha\text{-MgH}_2$ and TMH_2 as shown in Fig. 4. The bonding in MgH_2 is dominantly ionic; occupied hydrogen orbitals give the main contribution to the valence states, whereas the conduction bands have a significant contribution from the Mg orbitals.⁶⁰ As usual, ionic bonding between main group elements results in an insulator with a large band gap. In contrast, the transition-metal dihydrides are metallic, as demonstrated by Fig. 4. The peak in the DOS at low energy, i.e., between -9 and -2 eV in ScH_2 to between -12 and -4 eV in CrH_2 , is dominated by hydrogen states. The broad peak around the Fermi level consists of transition-metal d states. It suggests that bonding in TMH_2 is at least partially ionic. The TM s electrons are transferred to the H atoms, whereas the d electrons largely remain on the TM atoms. The DOSs of TMH_2 , with $\text{TM} = \text{Sc}, \text{Ti}, \text{V}, \text{ and } \text{Cr}$, are very similar in shape. As the number of d electrons increases from one in Sc to four in Cr, the Fermi level moves up the d

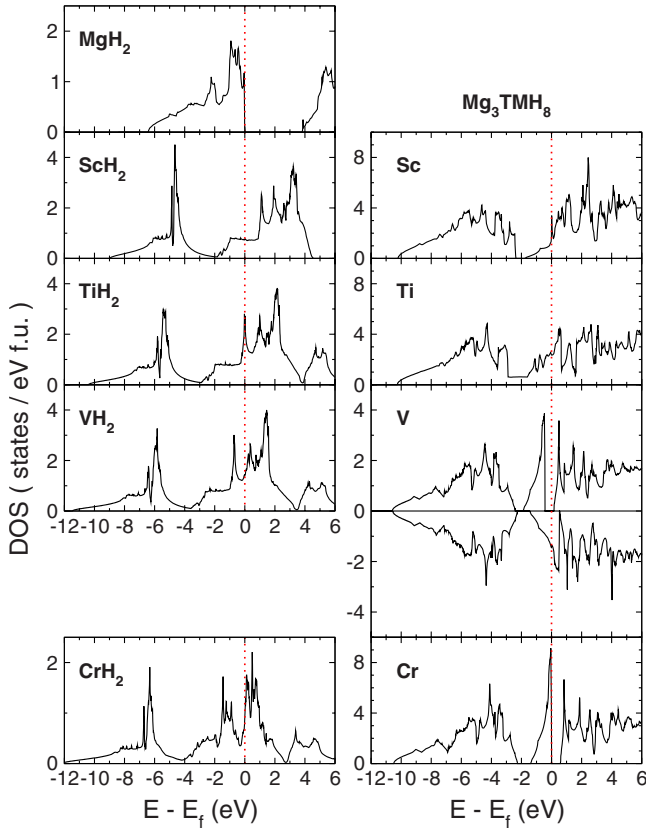


FIG. 4. (Color online) Densities of states of MgH_2 and TMH_2 (left column), and of $\text{Mg}_{0.75}\text{TM}_{0.25}\text{H}_2$ (right column) for $\text{TM}=\text{Sc}$, Ti , V , and Cr . For CrH_2 the nonmagnetic DOS is given for simplicity reasons; CrH_2 is antiferromagnetic (see text).

band in this series. As the DOS at the Fermi level increases, it enhances the probability of a magnetic instability. Indeed we find CrH_2 to be antiferromagnetic with a magnetic moment of $1.5\mu_B$ on the Cr atoms. The antiferromagnetic ordering is 51 meV/f.u. more stable than the ferromagnetic ordering, which is 7 meV/f.u. more stable than the nonpolarized solution. In the other TMH_2 we do not find magnetic effects.

Additional information on the type of bonding can be obtained from a Bader charge analysis.⁶¹ In $\alpha\text{-MgH}_2$ the Bader charges are $Q_{\text{Mg}}=+1.59e$ (and $Q_{\text{H}}=-0.80e$ since the compound is neutral), which confirms that this compound is dominantly ionic. The results for TMH_2 are shown in Table II. They indicate that the ionicity in ScH_2 is comparable to that in MgH_2 . Furthermore, the ionicity decreases along the series Sc , Ti , V , and CrH_2 . Comparison to Table I shows that the decrease in ionicity correlates with a decrease in formation enthalpy.

These results on the simple hydrides help us to analyze the electronic structure and bonding in $\text{Mg}_x\text{TM}_{(1-x)}\text{H}_2$. We show results for the fluorite structure only since that is the more stable structure over most of the composition range. As an example, Fig. 4 shows the calculated DOSs of $\text{Mg}_{0.75}\text{TM}_{0.25}\text{H}_2$. One can qualitatively interpret these DOSs as a superposition of the DOSs of MgH_2 and TMH_2 . The bonding states at low energy, comprising the first broad peak in the DOS, consist mainly of filled hydrogen states. The peaks close to the Fermi level are dominated by TM d states.

TABLE II. Bader charge analysis of TMH_2 and $\text{Mg}_{0.75}\text{TM}_{0.25}\text{H}_2$. All charges Q are given in units of e .

TM	TMH_2		$\text{Mg}_{0.75}\text{TM}_{0.25}\text{H}_2$	
	Q_{TM} (e)	Q_{H} (e)	Q_{TM} (e)	Q_{H} (e)
Sc	+1.51	-0.75	+1.57	-0.80
Ti	+1.17	-0.59	+1.18	-0.76
V	+1.09	-0.55	+0.98	-0.73
Cr	+0.89	-0.45	+0.68	-0.69

The Fermi level moves up the d band through the series Sc , Ti , V , and Cr . At higher energy we find the (unoccupied) Mg s states. The basic structure of the DOSs remains the same for all compositions $\text{Mg}_x\text{TM}_{(1-x)}\text{H}_2$. As x increases the TM d contribution of course decreases. In addition, the TM d peak becomes narrower with increasing x , as the distance between the TM atoms increases.

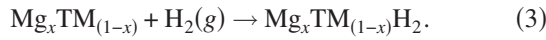
Narrowing of the d peak can give rise to magnetic instabilities. The tendency to such instabilities increases along the series Sc , Ti , V , and Cr . The development of nonzero magnetic moments of course strongly depends upon the structure. Nevertheless, for $\text{Mg}_x\text{Sc}_{(1-x)}\text{H}_2$ and $\text{Mg}_x\text{Ti}_{(1-x)}\text{H}_2$ we see a tendency to form magnetic moments on the TMs only if $x \geq 0.8$. For $\text{Mg}_x\text{V}_{(1-x)}\text{H}_2$ this occurs if $x \geq 0.5$, and for $\text{Mg}_x\text{Cr}_{(1-x)}\text{H}_2$ one can find magnetic instabilities over the whole composition range. Most of the structures have a finite DOS at the Fermi level, which might indicate a metallic behavior. However, one cannot conclude this on the basis of a DOS alone but should also critically evaluate possible localization and on-site correlation effects. There are a few exceptions. In particular cases low spin states can be more stable, such as for $\text{Mg}_{0.75}\text{Cr}_{0.25}\text{H}_2$ in the fluorite structure. Cubic crystal-field splitting by the hydrogens surrounding the Cr atom results in a gap between e_g and t_{2g} states, with the e_g states being lowest in energy. The latter are filled by the four d electrons of Cr, which makes this particular structure insulating (see Fig. 4). The DOS of $\text{Mg}_{0.75}\text{V}_{0.25}\text{H}_2$ in the fluorite structure is explained by the same mechanism. However, as V only has three d electrons, each V atom obtains a magnetic moment of $1\mu_B$. The distance between the TM atoms is fairly large in most compositions that have nonzero magnetic moments, which suggests a small magnetic coupling between the TM atoms, a low Néel or Curie temperature, and paramagnetic behavior at room temperature. Exceptions are the Cr compounds with a substantial amount of Cr, as discussed above.

A Bader charge analysis of $\text{Mg}_x\text{TM}_{(1-x)}\text{H}_2$ can be made, similar to the simple hydrides. For all compositions $Q_{\text{Mg}} \approx +1.6e$, i.e., close to the value found in $\alpha\text{-MgH}_2$. As an example, the Bader charges on the TM and H atoms in $\text{Mg}_{0.75}\text{TM}_{0.25}\text{H}_2$ are given in Table II. The charge on the TM atoms decreases along the series Sc , Ti , V , and Cr as in the simple hydrides but compared to the latter, it is somewhat smaller on V and Cr. The charges on the H atoms in $\text{Mg}_{0.75}\text{TM}_{0.25}\text{H}_2$ are roughly the proportional average of the charges on the H atoms in MgH_2 and TMH_2 . The charge

analysis of the $\text{Mg}_x\text{TM}_{(1-x)}\text{H}_2$ compounds is consistent with the bonding picture extracted from the DOSs.

IV. DISCUSSION

We discuss to what extent the Mg-TM alloys are suitable as hydrogen storage materials. The formation enthalpies of $\text{Mg}_x\text{TM}_{(1-x)}\text{H}_2$ are shown in Fig. 3. Lightweight materials require a high content of magnesium but to have a stable fluorite structure it should not exceed the critical composition x_c , as discussed in Sec. III A. We focus upon the composition $\text{Mg}_{0.75}\text{TM}_{0.25}\text{H}_2$ in the following discussion. The calculated formation enthalpies are -0.83 , -0.59 , -0.43 and -0.30 eV/f.u. for TM=Sc, Ti, V, and Cr, respectively. For applications the binding enthalpy of hydrogen in the lattice should be ≤ 0.4 eV/ H_2 ,²⁻⁴ which indicates that the Sc and Ti compounds are too stable. The formation enthalpies of the V and Cr compounds could be in the right range. However, the parameter that is most relevant for hydrogen storage is the hydrogenation enthalpy. Assuming that the alloy does not dissociate upon dehydrogenation, the hydrogenation enthalpy corresponds the reaction



To assess the hydrogenation enthalpy, one can break down the formation enthalpy associated with Eq. (1) into components, similar to the decomposition used in Ref. 37. We write the formation enthalpy as a sum of three terms. (i) The enthalpy required to make the Mg-TM alloy in the fcc structure from the elements in their most stable form. (ii) The energy required to expand the fcc lattice in order to incorporate the hydrogen atoms. (iii) The energy associated with inserting the hydrogen atoms. The results of this decomposition for $\text{Mg}_{0.75}\text{TM}_{0.25}\text{H}_2$ are given in Fig. 5. To facilitate the discussion, a similar decomposition is shown for the simple hydrides, where (i) only consists of transforming the pure metal into the fcc structure. In contrast to Ref. 37, we use the spin-polarized fcc alloy for calculating the contributions (i) and (ii) as this will make the extraction of the hydrogenation enthalpy easier. In the cases where the magnetic moment is nonzero, we study both ferromagnetic and antiferromagnetic orderings. As for the simple hydrides, Cr compounds generally have an antiferromagnetic ordering.

The lattice expansion energy (ii) of the compounds $\text{Mg}_{0.75}\text{TM}_{0.25}\text{H}_2$ is ≤ 0.1 eV for all TMs [see Fig. 5(b)]. It is in fact comparable to that of pure Mg [see Fig. 5(a)]. At the composition $\text{Mg}_{0.75}\text{TM}_{0.25}\text{H}_2$, the effect on the energy of changing the unit-cell volume is dominated by Mg. For these compounds the lattice expansion only plays a minor role in the formation energy, in contrast to the simple hydrides, where the lattice expansion gives a significant contribution. The hydrogen insertion energies (iii) are also remarkably similar for the Sc, Ti, and V compounds. Again this is in sharp contrast to the corresponding energies for the simple hydrides, which strongly depend on the TM. The hydrogen insertion energies for the compounds are in fact similar to that of pure Mg. At the composition $\text{Mg}_{0.75}\text{TM}_{0.25}\text{H}_2$ also this energy is then dominated by Mg. Only the compound $\text{Mg}_{0.75}\text{Cr}_{0.25}\text{H}_2$ has a somewhat smaller hydrogen insertion

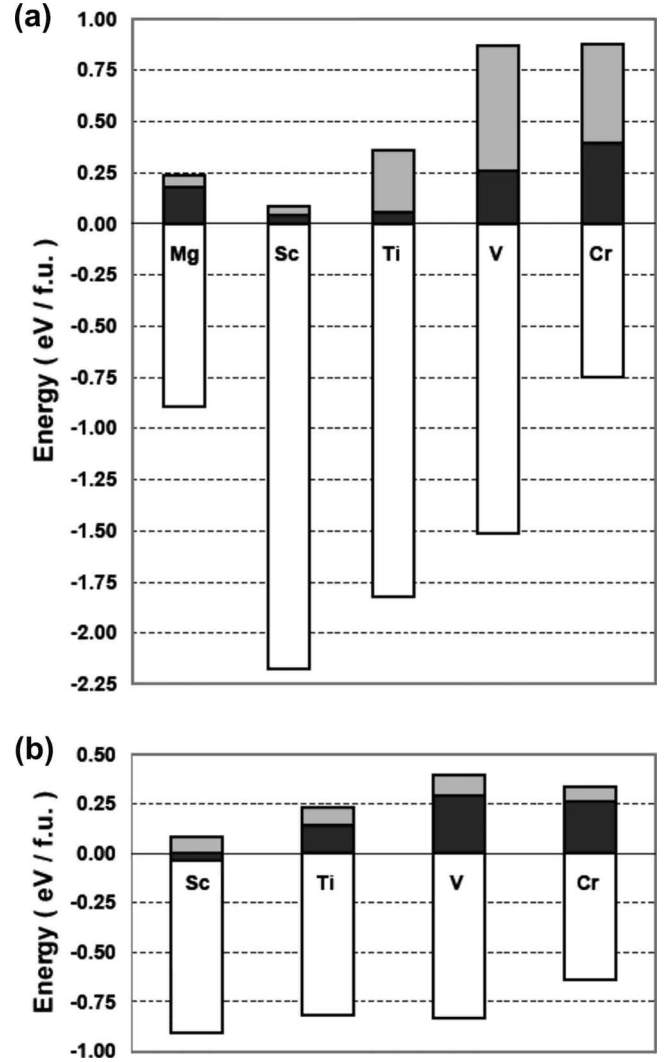


FIG. 5. Decomposition of the formation energy into (i) the formation energy of the spin-polarized fcc metal $\text{Mg}_{0.75}\text{TM}_{0.25}$ (black), (ii) the lattice expansion energy (gray), and (iii) the hydrogen insertion energy (white); (a) the simple hydrides MgH_2 and TMH_2 ; (b) $\text{Mg}_{0.75}\text{TM}_{0.25}\text{H}_2$.

energy. The reason for this is that the energy gained by magnetic ordering of the alloy $\text{Mg}_{0.75}\text{Cr}_{0.25}$ is relatively high, as compared to the other compounds. This contribution stabilizes the alloy with respect to the hydride, which is nonmagnetic.

The formation enthalpy of the fcc alloys $\text{Mg}_{0.75}\text{TM}_{0.25}$ (i) shows the largest variation as a function of the TM, relative to the contributions (ii) and (iii). Whereas the alloy formation energy is negative for TM=Sc, indicating that this alloy is stable, it is positive for Ti, V, and Cr, meaning that these alloys are unstable. This result agrees with the experimental finding that, of the Mg-TM alloys considered here, only a stable Mg-Sc alloy exists in bulk form. The substantial increase in the alloy formation enthalpy in the series Sc, Ti, and V is largely responsible for the variation in the formation energy of the corresponding hydrides $\text{Mg}_{0.75}\text{TM}_{0.25}\text{H}_2$. The alloy formation energy of $\text{Mg}_{0.75}\text{Cr}_{0.25}$ is similar to that of $\text{Mg}_{0.75}\text{V}_{0.25}$ due to a relatively high spin-polarization energy, as discussed in the previous paragraph.

The hydrogenation enthalpy according to Eq. (3) can be determined by summing the contributions (ii) and (iii) of Fig. 5. Since the most stable structure of the alloys is not always the fcc structure, one should however subtract the energy required to convert the alloys from their most stable structure to an fcc structure. We find that, for instance, for $\text{Mg}_{0.75}\text{Ti}_{0.25}$ the fcc structure is 0.04 eV/f.u. less stable than the hcp structure. Indeed thin-film experiments on $\text{Mg}_x\text{Ti}_{(1-x)}$ yield an hcp structure.^{19,23} For $\text{Mg}_{0.75}\text{Sc}_{0.25}$ the fcc structure is more stable than the hcp structure by 0.05 eV/f.u..

The calculated hydrogenation enthalpy of $\text{Mg}_{0.75}\text{Sc}_{0.25}$ is -0.79 eV/f.u., in good agreement with the experimental value of -0.81 eV/f.u..¹⁹ The calculated hydrogenation enthalpy of $\text{Mg}_{0.75}\text{Ti}_{0.25}$ is -0.76 eV/f.u., which is in good agreement with the experimental value of -0.81 eV/f.u. of Ref. 26, obtained if the thin-film correction suggested there is included. These hydrogenation enthalpies are remarkably similar to that of pure Mg, strongly suggesting that alloying Mg with these TMs does not improve this energy as compared to pure Mg. The most stable structures of $\text{Mg}_{0.75}\text{TM}_{0.25}$, with TM=V and Cr, are not known but judging from the Sc and Ti compounds the energy difference between the fcc and the most stable structures will be small. Neglecting this energy difference, upper bounds for the hydrogenation enthalpies of $\text{Mg}_{0.75}\text{V}_{0.25}$ and $\text{Mg}_{0.75}\text{Cr}_{0.25}$ are -0.72 and -0.57 eV/f.u., respectively. Again this indicates that alloying Mg with these TMs does not improve the hydrogenation enthalpy substantially.

V. SUMMARY

In summary, we have studied the structure and stability of $\text{Mg}_x\text{TM}_{(1-x)}\text{H}_2$, with TM=Sc, Ti, V, and Cr, compounds by first-principles calculations. We find that for $x < x_c \approx 0.8$ the fluorite structure is more stable than the rutile structure, whereas for $x > x_c$ the rutile structure is more stable. The density of states of these compounds is characterized by the

valence bands being dominated by contributions from the hydrogen atoms, whereas the TMs have partially occupied d states around the Fermi level. As x increases and/or one moves down the TM series, the tendency for magnetic instabilities increases.

The formation enthalpy of $\text{Mg}_x\text{TM}_{(1-x)}\text{H}_2$ can be tuned over a substantial range, i.e., $0-2$ eV/f.u., by varying TM and x . To a large part this reflects the variation in the formation enthalpy of the alloy $\text{Mg}_x\text{TM}_{(1-x)}$, however. Assuming that the alloys do not decompose upon dehydrogenation, the hydrogenation enthalpy then shows much less variation. For compounds with a high magnesium content ($x=0.75$), it is close to that of pure Mg. Introducing a third metallic element may however be used to significantly improve the thermodynamics of (de)hydrogenation. The study of ternary alloys of Mg with transition metals and/or simple metals is actively pursued at present.^{24,62-64}

The phase transition from the rutile to the fluorite structure in $\text{Mg}_x\text{TM}_{(1-x)}\text{H}_2$, if x falls below the critical composition x_c , correlates with the experimentally observed speeding up of the (de)hydrogenation kinetics in these compounds. A discussion of the kinetics is beyond the scope of the present paper. However, our preliminary calculations indicate that, even in MgH_2 , hydrogen diffusion in the cubic (fluorite derived) β - MgH_2 phase is much faster than in the rutile α - MgH_2 phase both through a smaller formation energy for a hydrogen vacancy as well as through a lower barrier for vacancy diffusion.

ACKNOWLEDGMENTS

This work is part of the research programs of Advanced Chemical Technologies for Sustainability (ACTS) and the Stichting voor Fundamenteel Onderzoek der Materie (FOM). The use of supercomputer facilities was sponsored by the Stichting Nationale Computerfaciliteiten (NCF). These institutions are financially supported by Nederlandse Organisatie voor Wetenschappelijk Onderzoek (NWO).

- ¹R. Coontz and B. Hanson, in *Toward a Hydrogen Economy*, special issue of Science **305**, 957 (2004).
- ²A. Züttel, Mater. Today **6**, 24 (2003).
- ³A. Züttel, Naturwiss. **91**, 157 (2004).
- ⁴L. Schlapbach and A. Züttel, Nature (London) **414**, 353 (2001).
- ⁵B. Bogdanovic, M. Felderhoff, S. Kaskel, A. Pommerin, K. Schlichte, and F. Schuth, Adv. Mater. (Weinheim, Ger.) **15**, 1012 (2003).
- ⁶J. F. Stampfer, Jr., C. E. Holley, Jr., and J. F. Suttle, J. Am. Chem. Soc. **82**, 3504 (1960).
- ⁷J. Huot, G. Liang, and R. Schulz, Appl. Phys. A: Mater. Sci. Process. **72**, 187 (2001).
- ⁸W. Grochala and P. P. Edwards, Chem. Rev. (Washington, D.C.) **104**, 1283 (2004).
- ⁹A. Zaluska, L. Zaluski, and J. O. Ström-Olsen, Appl. Phys. A: Mater. Sci. Process. **72**, 157 (2001).
- ¹⁰M. Dornheim, N. Eigen, G. Barkhordarian, T. Klassen, and R.

- Bormann, Adv. Eng. Mater. **8**, 377 (2006).
- ¹¹W. Li, C. Li, H. Ma, and J. Chen, J. Am. Chem. Soc. **129**, 6710 (2007).
- ¹²R. W. P. Wagemans, J. H. van Lenthe, P. E. de Jongh, A. J. van Dillen, and K. P. de Jong, J. Am. Chem. Soc. **127**, 16675 (2005).
- ¹³J. F. Pelletier, J. Huot, M. Sutton, R. Schulz, A. R. Sandy, L. B. Lurio, and S. G. J. Mochrie, Phys. Rev. B **63**, 052103 (2001).
- ¹⁴F. von Zeppelin, H. Reule, and M. Hirscher, J. Alloys Compd. **330-332**, 723 (2002).
- ¹⁵X. Yao, C. Wu, A. Du, G. Q. Lu, H. Cheng, S. C. Smith, J. Zou, and Y. He, J. Phys. Chem. B **110**, 11697 (2006).
- ¹⁶P. H. L. Notten, M. Ouwerkerk, H. van Hal, D. Beelen, W. Keur, J. Zhou, and H. Feil, J. Power Sources **129**, 45 (2004).
- ¹⁷R. A. H. Niessen and P. H. L. Notten, Electrochem. Solid-State Lett. **8**, A534 (2005a).
- ¹⁸R. A. H. Niessen and P. H. L. Notten, J. Alloys Compd. **404-406**, 457 (2005).

- ¹⁹W. P. Kalisvaart, R. A. H. Niessen, and P. H. L. Notten, *J. Alloys Compd.* **417**, 280 (2006).
- ²⁰R. A. H. Niessen, P. Vermeulen, and P. H. L. Notten, *Electrochim. Acta* **51**, 2427 (2006).
- ²¹P. Vermeulen, R. A. H. Niessen, and P. H. L. Notten, *Electrochem. Commun.* **8**, 27 (2006a).
- ²²D. M. Borsa, A. Baldi, M. Pasturel, H. Schreuders, B. Dam, R. Griessen, P. Vermeulen, and P. H. L. Notten, *Appl. Phys. Lett.* **88**, 241910 (2006).
- ²³D. M. Borsa, R. Gremaud, A. Baldi, H. Schreuders, J. H. Rector, B. Kooi, P. Vermeulen, P. H. L. Notten, B. Dam, and R. Griessen, *Phys. Rev. B* **75**, 205408 (2007).
- ²⁴P. Vermeulen, E. F. M. J. van Thiel, and P. H. L. Notten, *Chem.-Eur. J.* **13**, 9892 (2007).
- ²⁵W. P. Kalisvaart, H. J. Wondergem, F. Bakker, and P. H. L. Notten, *J. Mater. Res.* **22**, 1640 (2007).
- ²⁶R. Gremaud, C. P. Broedersz, D. M. Borsa, A. Borgschulte, P. Mauron, H. Schreuders, J. H. Rector, B. Dam, and R. Griessen, *Adv. Mater. (Weinheim, Ger.)* **19**, 2813 (2007).
- ²⁷K. H. J. Buschow, P. C. P. Bouten, and A. R. Miedema, *Rep. Prog. Phys.* **45**, 937 (1982).
- ²⁸J. P. Perdew, K. Burke, and M. Ernzerhof, *Phys. Rev. Lett.* **77**, 3865 (1996).
- ²⁹P. E. Blöchl, *Phys. Rev. B* **50**, 17953 (1994).
- ³⁰G. Kresse and D. Joubert, *Phys. Rev. B* **59**, 1758 (1999).
- ³¹G. Kresse and J. Hafner, *Phys. Rev. B* **47**, 558 (1993).
- ³²G. Kresse and J. Furthmüller, *Phys. Rev. B* **54**, 11169 (1996).
- ³³M. Methfessel and A. T. Paxton, *Phys. Rev. B* **40**, 3616 (1989).
- ³⁴P. E. Blöchl, O. Jepsen, and O. K. Andersen, *Phys. Rev. B* **49**, 16223 (1994).
- ³⁵K. P. Huber and G. Herzberg, *Molecular Spectra and Molecular Structure* (Van Nostrand Reinhold, New York, 1979), Chap. IV.
- ³⁶J. D. Cox, D. D. Wagman, and V. A. Medvedev, *CODATA Key Values for Thermodynamics* (Hemisphere, New York, 1989).
- ³⁷K. Miwa and A. Fukumoto, *Phys. Rev. B* **65**, 155114 (2002).
- ³⁸C. Wolverton, V. Ozolins, and M. Asta, *Phys. Rev. B* **69**, 144109 (2004).
- ³⁹L. Zhang, Y. Wang, T. Cui, Y. Li, Z. He, Y. Ma, and G. Zou, *Phys. Rev. B* **75**, 144109 (2007).
- ⁴⁰M. Bortz, B. Bertheville, G. Bottger, and K. Yvon, *J. Alloys Compd.* **287**, L4 (1999).
- ⁴¹W. M. Mueller, J. P. Blackledge, and G. G. Libowitz, *Metal Hydrides* (Academic, New York, 1968).
- ⁴²P. Villars, L. D. Calvert, and W. B. Pearson, *Pearson's Handbook of Crystallographic Data for Intermetallic Phases* (ASM, Materials Park, OH, 1991).
- ⁴³C. A. Snavely and D. A. Vaughan, *J. Am. Chem. Soc.* **71**, 313 (1949).
- ⁴⁴M. Lacroche, W. P. Kalisvaart, and P. H. L. Notten, *J. Solid State Chem.* **179**, 3024 (2006).
- ⁴⁵P. C. M. M. Magusin, W. P. Kalisvaart, P. H. L. Notten, and R. A. van Santen, *Chem. Phys. Lett.* **456**, 55 (2008).
- ⁴⁶P. Vermeulen, R. A. H. Niessen, D. M. Borsa, B. Dam, R. Griessen, and P. H. L. Notten, *Electrochem. Solid-State Lett.* **9**, A520 (2006b).
- ⁴⁷G. Liang, J. Huot, S. Boily, A. V. Neste, and R. Schulz, *J. Alloys Compd.* **292**, 247 (1999).
- ⁴⁸J. L. Bobet, C. Even, Y. Nakamura, E. Akiba, and B. Darriet, *J. Alloys Compd.* **298**, 279 (2000).
- ⁴⁹G. Liang and R. Schulz, *J. Mater. Sci.* **38**, 1179 (2003).
- ⁵⁰Y. J. Choi, J. Lu, H. Y. Sohn, and Z. Z. Fang, *J. Power Sources* **180**, 491 (2008).
- ⁵¹D. Kyoï, T. Sato, E. Rönnebro, N. Kitamura, A. Ueda, M. Ito, S. Katsuyama, S. Hara, D. Noréus, and T. Sakai, *J. Alloys Compd.* **372**, 213 (2004a).
- ⁵²D. Kyoï, E. Rönnebro, N. Kitamura, A. Ueda, M. Ito, S. Katsuyama, and T. Sakai, *J. Alloys Compd.* **361**, 252 (2003).
- ⁵³D. Kyoï *et al.*, *J. Alloys Compd.* **375**, 253 (2004b).
- ⁵⁴E. Rönnebro, D. Kyoï, H. Blomqvist, D. Noréus, and T. Sakai, *J. Alloys Compd.* **368**, 279 (2004).
- ⁵⁵E. Rönnebro, D. Kyoï, A. Kitano, Y. Kitano, and T. Sakai, *J. Alloys Compd.* **404-406**, 68 (2005).
- ⁵⁶A. V. Ruban, S. I. Simak, S. Shallcross, and H. L. Skriver, *Phys. Rev. B* **67**, 214302 (2003).
- ⁵⁷S. Er, M. van Setten, G. de Wijs, and G. Brocks (unpublished).
- ⁵⁸P. Vajeeston, P. Ravindran, A. Kjekshus, and H. Fjellvåg, *Phys. Rev. Lett.* **89**, 175506 (2002).
- ⁵⁹J. Hafner, *J. Phys. F: Met. Phys.* **15**, L43 (1985).
- ⁶⁰M. J. van Setten, V. A. Popa, G. A. de Wijs, and G. Brocks, *Phys. Rev. B* **75**, 035204 (2007).
- ⁶¹G. Henkelman, A. Arnaldsson, and H. Jónsson, *Comput. Mater. Sci.* **36**, 354 (2006).
- ⁶²M. J. van Setten, G. A. de Wijs, V. A. Popa, and G. Brocks, *Phys. Rev. B* **72**, 073107 (2005).
- ⁶³M. J. van Setten, G. A. de Wijs, and G. Brocks, *Phys. Rev. B* **76**, 075125 (2007).
- ⁶⁴C. P. Broedersz, R. Gremaud, B. Dam, R. Griessen, and O. M. Lovvik, *Phys. Rev. B* **77**, 024204 (2008).